Address correspondence to: Dr. Stephen Foster
North Dakota State University
Entomology Department
NDSU Dept 7650
PO Box 6050
Fargo, ND 58108-6050
U.S.A
Ph. 1-701-231-6444
Fax 1-701-231-8557
Email: stephen.foster@ndsu.edu

# Sex pheromone in the moth *Heliothis virescens* is produced as a mixture of two pools: de novo and via precursor storage in glycerolipids

Stephen P. Foster[1], Karin G. Anderson[1] and Jérôme Casas[2]

[1]Entomology Department, North Dakota State University,
PO Box 6050, Fargo, North Dakota 58108-6050, U.S.A
and
[2]Université de Tours, Institut de Recherche sur la Biologie de l'Insecte,
UMR CNRS 7261, 37200 Tours, FRANCE

**Abstract**

Most species of moths use a female-produced volatile sex pheromone, typically produced via de novo fatty acid synthesis in a specialized gland, for communication among mates. While de novo biosynthesis of pheromone (DNP) is rapid, suggesting transient precursor acids, substantial amounts of pheromone precursor (and other) acids are stored, predominantly in triacylglycerols in the pheromone gland. Whether these stored acids are converted to pheromone later or not has been the subject of some debate. Using a tracer/tracee approach, in which we fed female *Heliothis virescens* U-$^{13}$C-glucose, we were able to distinguish two pools of pheromone, in which precursors were temporally separated (after and before feeding on labeled glucose): DNP synthesized from a mixed tracer/tracee acetyl CoA pool after feeding, and pheromone made from precursor acids primarily synthesized before feeding, which we call recycled precursor fat pheromone (RPP). DNP titer varied from high (during scotophase) to low (photophase) and with presence/absence of pheromone biosynthesis activating neuropeptide (PBAN), in accord with native pheromone titer previously observed. By contrast, RPP was constant throughout the photoperiod and did not change with PBAN presence/absence. The amount of RPP (6.3-10.3 ng/female) was typically much lower than that of DNP, especially during the scotophase (peak DNP, 105 ng/female). We propose an integral role for stored fats in pheromone biosynthesis, in which they are hydrolyzed and re-esterified throughout the photoperiod, with a small proportion of liberated precursor acyl CoAs being converted to pheromone. During the sexually active period, release of PBAN results in increased flux of glucose (from trehalose) and hydrolyzed acids entering the

mitochondria, producing acetyl CoA precursor for de novo fat and pheromone biosynthesis.

**Keywords:** Chemical communication; stable isotope; tracer/tracee; mass isotopomer distribution analysis; Noctuidae; Lepidoptera.

## 1. Introduction

The use of volatile sex pheromones to bring mates together for copulation is prevalent among the group of insects known as moths (order: Lepidoptera) (Allison and Cardé, 2016). Female moths produce and/or release a sex pheromone, typically a blend of closely related chemicals, from a specialized gland usually located on the intersegmental membrane between the 8$^{th}$ and 9$^{th}$ abdominal segments (Ma and Ramaswamy, 2003). Elevated production and release of pheromone typically occur during a defined temporal period of the day, when a species is sexually active (Groot, 2014). In many species of moths, the period of elevated production is governed by the release of the pheromone biosynthesis-activating neuropeptide (PBAN) from the corpora cardiaca into the hemolymph (Blomquist et al., 2011; Rafaeli and Jurenka, 2003).

Species of moths that biosynthesize so-called "Type 1" sex pheromone components do so by a route involving rapid de novo fatty acid synthesis from acetyl CoA, followed by desaturation and/or cytosolic β-oxidation of the alkyl chain and modification of the carboxyl group to an alcohol, aldehyde or acetate ester (Ando et al., 2004; Blomquist et al., 2011; Foster, 2016). De novo biosynthesis of pheromone requires a supply of acetyl CoA precursor, which is provided by glycolysis/pyruvate oxidation of hemolymph trehalose, and mitochondrial β-oxidation of fatty acids from glandular glycerolipids (Foster and Anderson, 2015). In addition to providing fatty acids for β-oxidation, glandular glycerolipids also contain relatively substantial amounts of pheromone precursor acids, which may or may not subsequently be converted to pheromone (Bjostad et al., 1987; Fang et al., 1995; Foster, 2005b; Matsumoto, 2010). For instance, in the

92 silkworm moth, *Bombyx mori*, which uses a single component (bombykol) as its sex
93 pheromone, triacylglycerol stores of pheromone precursor acids accumulate throughout
94 the non-sexually active period. These are then hydrolyzed and reduced to pheromone
95 following release of PBAN during the sexually active period (Matsumoto, 2010). By
96 contrast, species such as the redbanded leafroller, *Argyrotaenia velutinana*, and the
97 European corn borer, *Ostrinia nubilalis,* which use highly specific ratios of geometric
98 isomers as pheromone components, may have a preponderance of the precursor acid of
99 the minor pheromone component over that of the major component stored in
100 glycerolipids (Bjostad et al., 1981; Foster, 2004). This suggests that there is little release
101 and conversion of these acids directly to pheromone. In these cases, fatty acids may still
102 be hydrolyzed from glycerolipids by lipases for β-oxidation, but the much greater
103 abundances of other acids will likely result in a relatively low release of pheromone
104 precursor acids with an insignificant effect on the ratio of pheromone components
105 produced.
106
107 Sex pheromone biosynthesis and glandular glycerolipids have been extensively studied in
108 the moth *Heliothis virescens* (Fabricius) (family: Noctuidae) (Choi et al., 2005; Foster
109 and Anderson, 2011; Foster, 2005a, b; Foster and Anderson, 2012; Groot et al., 2016;
110 Hagström et al., 2013), which uses a blend of (*Z*)-11-hexadecenal (Z11-16:Ald) and (*Z*)-
111 9-tetradecenal as its sex pheromone (Roelofs et al., 1974). Recently, using the stable
112 isotope tracer-tracee method of mass isotopomer distribution analysis (MIDA; Hellerstein
113 and Neese, 1999), we established that females use a roughly 2:1 ratio of carbohydrate
114 (from hemolymph trehalose) to stored fats as nutrients for production of acetyl CoA

115 during de novo pheromone biosynthesis (Foster and Anderson, 2015). However, we
116 noticed that a significant portion of the unlabeled pheromone could not have been
117 produced from the tracer/tracee pool of acetyl CoA used for de novo-produced
118 pheromone (DNP). We concluded that this unlabeled pheromone must arise from a
119 distinct precursor pool, containing no labeled acetyl CoA, most likely from pheromone
120 precursor acids, specifically (*Z*)-11-hexadecenoate (Z11-16:Acyl), hexadecanoate
121 (16:Acyl), and octadecanoate (18:Acyl), synthesized and stored before introduction of the
122 tracer. These stored acids may be converted directly, without mitochondrial β-oxidation,
123 to pheromone (Choi et al., 2005).
124
125 This result suggested that recycling of stored precursor fats converted directly to
126 pheromone ("recycled precursor fat pheromone"; RPP) might be an important contributor
127 to pheromone production in *H. virescens*, particularly at different times of the
128 photoperiod or with increased age. For example, most of the pheromone produced early
129 in the scotophase, and released first by females, could be produced via this route before
130 DNP production contributed more. Since we are developing a quantitative model to
131 describe pheromone production and release in *H. virescens*, we sought to (i) characterize
132 the overall production pathway structure, (ii) estimate some of its parameters, in
133 particular the relative contributions of DNP and RPP, (iii) determine whether their
134 contributions were time dependent with respect to photoperiod and age, and (iv)
135 determine whether PBAN influenced the production of RPP and DNP, as it does for
136 native pheromone (Eltahlawy et al., 2007; Groot et al., 2005).
137

## 2. Methods and Materials

### *2.1. Insects*

*Heliothis virescens* were from a colony maintained at NDSU, Fargo, but originating from a colony previously established at USDA-ARS BRL, Fargo, and recently supplemented with insects supplied by Dr. F.A. Gould (North Carolina State University, Raleigh, NC). Larvae were reared at 25ºC under a 16:8 L:D photoperiod and fed on a wheatgerm-casein diet until they pupated, after which they were sexed and the two sexes maintained separately under the same environmental conditions as larvae.

Adults were collected daily and categorized as 1–d-old the day after eclosion, 2-d-old, two days after eclosion, etc. Prior to the start of an experiment, adults were starved and denied access to any liquids. The stable isotope tracer was introduced by allowing an adult to feed on 25 µl of a 10% (w/v) aqueous solution of U-$^{13}$C-glucose (99%; Cambridge Isotope Laboratories, Cambridge, MA) as a drop on a watch glass; only females that consumed the full amount were used in experiments. The labeled glucose, absorbed rapidly into hemolymph trehalose, undergoes glycolysis and oxidation to generate $^{13}C_{1,2}$-acetyl-CoA tracer, which is incorporated into pheromone and gland fats (Foster and Anderson, 2011; Foster and Anderson, 2012).

### *2.2. Extraction, Derivatization and Chemical Analysis*

The pheromone gland of a female was extruded by applying gentle force to the abdomen and then excised with fine forceps. For pheromone extraction, the gland was placed in 5

μl of *n*-heptane containing 25 ng of (*Z*)-11-tetradecenal (Z11-14:Ald) as an internal standard and allowed to extract for at least 1 h at ambient temperature before analysis. For fatty acid extraction, the gland was placed in 50 μl of a 2:1 mixture of $CH_2Cl_2$: MeOH along with 250 ng of tripentadecanoin (Sigma-Aldrich, St Louis, MO) as an internal standard, and allowed to extract at -15°C overnight.

The pheromone extract was injected into an Agilent 7890/5978A gas chromatograph/mass spectrometer (GC/MS), whereas the fat extract was subjected to base methanolysis to generate fatty acid methyl esters (FAMEs). Briefly, after extraction, the solvent was decanted and removed by a gentle stream of nitrogen. Then, 50 μl of 0.5 M methanolic KOH was added and allowed to react for 1 h at ambient temperature before 50 μl of 1 M HCl (aq) was added along with 25 μl of heptane. The solution was subjected to rapid vortexing for 30 sec., before the heptane layer (top) was decanted and injected in the GC/MS for analysis.

The GC used helium at a constant flow of 1.5 $ml.min^{-1}$ as carrier gas, and splitless injection. The column was a 30 m x 0.25 mm i.d x 250 μm film thickness ZBWax (Phenomenex, Torrance, CA) and the oven temperature was programmed from 80°C (delay of 1 min) to 180 at 15°$C.min^{-1}$, then to 190 at 5°$C.min^{-1}$, and finally to 220 at 20°$C.min^{-1}$. The MS was operated with electron impact ionization at 70 eV and used in the single ion monitoring mode. The MS source and quadrupole were set at 230°C and 150°C, respectively.

For the pheromone analyses, the following *m/z* were monitored: 192 for the internal standard ( Z11-14:Ald), 220, 222, and 224, for Z11-16:Ald (we only analyzed the major pheromone component, as it comprises >90% of the mass of the pheromone and is biosynthesized similarly to the minor component Z9-14:Ald; Choi et al., 2005; Teal et al., 1986). The *m/z* 192 and 220 were monitored because they are ions [$(M-H_2O)^+$] of intact (unlabeled) carbon skeletons of Z11-14:Ald and Z11-16:Ald, respectively, and carry more ion current than their respective parent ions. The *m/z* 222 and 224 are the M+1 (+one $^{13}C_2$ unit) and M+2 (+two $^{13}C_2$ unit) isotopomers of Z11-16:Ald.

The FAMEs of Z11-16:Acyl and 16:Acyl were analyzed similarly by monitoring their molecular ions, namely *m/z* 268 (M+0 for Z11-16:Acyl), 270, (M+1 for Z11-16:Acyl, M+0 for 16:Acyl), 272 (M+2 for Z11-16:Acyl, M+1 for 16:Acyl) and 274 (M+2 for 16:Acyl), along with *m/z* 256 of the internal standard methyl pentadecanoate.

*2.3. Mass Isotopomer Distribution Analysis*

MIDA is a combinatorial approach to determine isotopic (precursor) enrichment in a monomeric pool used to synthesize a polymer, following the introduction of a stable isotope-labeled monomer (Hellerstein and Neese, 1992; Wolfe and Chinkes, 2005). It accomplishes this by measuring intensities of both unlabeled and labeled isotopomers of the polymer, while accounting for abundances of natural isotopes. The precursor enrichment, i.e., the proportion of labeled monomeric units in the resulting polymer, can be calculated using the pattern of isotopomers. An advantage of MIDA is that it is not subject to isotopic discrimination in the precursor pool (Hellerstein and Neese, 1999).

We used MIDA to calculate precursor enrichment following introduction of the tracer ($^{13}C_2$-acetyl CoA) formed after insects had fed on U-$^{13}$C-glucose. We analyzed females at least 16 h after they had fed, so that the precursor pool and pheromone or pheromone precursor acids were in isotopic equilibrium (Foster and Anderson, 2011; Foster and Anderson, 2012). To calculate precursor enrichment, tracer/tracee ratios (TTRs) of singly (M+1) and doubly (M+2) labeled (i.e., with one and two $^{13}C_2$ units, respectively) isotopomers were calculated for the acetyl CoA octomers Z11-16:Ald, Z11-16:Acyl and 16:Acyl as follows:

(1) $TTR(M+1) = (M+1/M+0)_{post} - (M+1/M+0)_{pre}$

(2) $TTR(M+2) = (M+2/M+0)_{post} - (M+2/M+0)_{pre} - dT_1 \times TTR(M+1)$

Where 'pre' and 'post' subscripts, respectively, refer to the intensities of isotopomers before and after tracer is introduced. We used theoretically calculated values of the pre intensities (using known natural isotopic abundances), rather than experimentally determined ones, as previously (Foster and Anderson, 2011; Foster and Anderson, 2012) we found little difference between the two. The term $dT_1$ is the contribution of the M+1 isotopomer spectrum to the M+2 isotopomer. Then, precursor enrichment ("*p*", in molar percent excess) of an octomer can be calculated by:

(3) $p = 2 \times [TTR(M+2)/TTR(M+1)] \div [7 + TTR(M+2)/TTR(M+1)]$

In order to calculate the amount of unlabeled pheromone not produced by de novo biosynthesis (i.e., RPP) after addition of the tracer, we used precursor enrichment to predict the entire isotopomer pattern (for all 9 isotopomers, M+0–8). Then, by using the

observed intensity of the M+2 isotopomer (minus any natural isotopic contributions from the M+0 and M+1 isotopomers), we calculated the expected intensity of the M+0 isotopomer produced via de novo synthesis from the labeled/unlabeled acetyl CoA pool. This was subtracted from the intensity of the observed M+0 isotopomer to allow the amount (relative to the internal standard) of RPP to be determined. Similarly, using the sum of all (nine) isotopomers expected for a given *p*, we calculated the amount of DNP. De novo-produced (i.e., labeled, including expected M+0 isotopomer, after U-$^{13}$C-glucose was ingested) and previously synthesized (unlabeled, before feeding) stored Z11-16:Acyl and 16:Acyl were calculated similarly.

*2.4. Isotopic fractionation*

To test whether quantification of both DNP and RPP pools was affected by significant isotopic fractionation from use of the $^{13}$C-tracer, we fed 1 d females either unlabeled (>99% pure and natural isotopic composition; Sigma-Aldrich, St Louis, MO) or $^{13}$C-labeled glucose at the end of the scotophase. The following day, at the beginning of the scotophase (i.e., 16 h later), we quantified the amount of unlabeled pheromone in females fed unlabeled glucose, and the amounts of DNP and RPP in females fed labeled glucose. The total amounts (i.e., DNP + RPP for females fed U-$^{13}$C-glucose vs total pheromone in females fed unlabeled glucose) for each treatment were compared.

*2.5. Effect of age and time of photoperiod*

We determined the amount of DNP and RPP in females of different ages and at different times during the scotophase, in order to test whether the respective amounts in the gland

253 varied through time. For this, we fed females of different ages (0, 1, 2, and 3 d) U-$^{13}$C-
254 glucose at the end of the scotophase and left them for at least 18 h before analyzing
255 pheromone at hour 2 of the scotophase (hereafter, hours of the photoperiod are referred to
256 as S2, P16, etc., with the letter indicating scotophase or photophase and the number the
257 hour of the respective period). Females fed at 1 d were analyzed more extensively,
258 starting at P14 of the subsequent photophase and then every 2 h throughout the
259 subsequent scotophase (i.e., when 2 d old). In addition, 1 d females were fed 6 h into their
260 first complete photophase (i.e., the photophase preceding the scotophase in which they
261 were analyzed every 2 h) and analyzed 24 h later (at P6). From 5–13 females were
262 analyzed for each time point.
263
264 *2.6. Effect of decapitation*
265 To test whether the amounts of DNP and RPP are influenced by the absence of PBAN,
266 we fed 1 d females U-$^{13}$C-glucose at the end of the scotophase and decapitated them 18 h
267 later (at Scot2). Decapitation stops PBAN reaching the pheromone gland and
268 consequently results in a rapid decrease in pheromone titer (Rafaeli and Jurenka, 2003).
269 We sampled females at 0 (immediately prior to decapitation), 0.25. 0.5, 1.0, 1.5, 2, 4, 6
270 and 24 h later. Five to eight females were analyzed at each time.
271
272 In the second part, 1 d females were fed U-$^{13}$C-glucose and then, in the following
273 scotophase (i.e., at least 16 h later) analyzed for total labeled (i.e., carbon chain
274 synthesized after introduction of the labeled glucose) and excess unlabeled (i.e., carbon
275 chain synthesized before introduction of the labeled glucose or from a pool of precursor

276 that was not derived from labeled glucose) FAMEs of Z11-16:Acyl and 16:Acyl. Three
277 groups of females were analyzed: (i) intact females at S0, (ii) intact females at S6, and
278 (iii) females decapitated at S0 and analyzed at S6.
279
280 *2.7. Effect of PBAN*
281 We conducted the complementary experiment to the previous one by injecting PBAN
282 into decapitated females and determining the effect on DNP and RPP. One-day-old
283 females were fed at the end of the scotophase and, immediately upon ingestion of the U-
284 $^{13}$C-glucose, decapitated. The decapitated females were then left for 18 h, at which time
285 they were either injected with 5 pmole of PBAN (HeZ; Bachem, Torrance, CA) in saline
286 (2.5 µl) or the same volume of saline (NaCl, 187.5 mmol.l$^{-1}$, KCl, 4.83 mmol.l$^{-1}$, $CaCl_2$,
287 2.61 mmol.l$^{-1}$, Hepes, 10 mmol.l$^{-1}$, pH=6.8). They were analyzed for DNP and RPP at 0
288 (only saline injected), 0.25, 0.5, 1.0, 1.5 and 4.0 h later.
289
290 A similar experimental approach was adopted for analysis of total labeled and excess
291 unlabeled FAMEs of Z11-16:Acyl and 16:Acyl, except females were analyzed at 0 (no
292 PBAN or saline injected), 0.5 and 4.0 h (for both saline- and PBAN-injected females).
293
294 *2.8. Statistical analyses*
295 For the effect of photoperiod and age, we used ANCOVA with RPP, DNP or precursor
296 enrichment as dependent variables, age as a covariate and time of photoperiod as a
297 categorical independent variable, after first checking normality and heteroscedasity of the
298 data. For all other data, we used ANOVA to test for differences, again after checking the

299 normality and heteroscedasity of the data, and tested differences among means by post-
300 hoc Tukey-Kramer HSD tests with $\alpha$ set at P = 0.05. In the decapitation experiment, we
301 made two temporal comparisons: the first was of RPP and DNP titers over the first 6 h of
302 decapitation, and the second was a binary comparison for both RPP and DNP titers just
303 prior to and 24 h after, decapitation.
304
305 **3. Results**
306
307 *3.1. Isotopic fractionation effect*
308 At the start of the scotophase, females fed unlabeled glucose the previous day had a mean
309 pheromone titer of 17.9±2.7 ng/female (N=10), whereas females fed U-$^{13}$C-glucose had a
310 mean total RPP+DNP titer of 22.2±3.5 ng/female (N=14); these means were not different
311 (ANOVA, $F_{1,22} = 0.86$, $p = 0.36$). Thus, any isotopic effects that occurred in the
312 biosynthesis of pheromone from U-$^{13}$C-glucose did not affect pheromone gland titer.
313
314 *3.2. Effect of photoperiod and age*
315 At all times of the photoperiod and all ages tested, females had substantial and reasonably
316 constant titers of RPP in the gland, varying from a mean of 6.3±1.7 to 10.3±1.4 ng/female
317 (Fig. 1a). ANCOVA, with amount of RPP as the dependent variable, showed no effect of
318 time of photoperiod ($F_{5,65} = 0.64$, $p = 0.67$), but an effect of age ($F_{1,65} = 5.59$, $p = 0.021$).
319 Essentially, the amount of RPP declined slightly with increasing age of female, but the
320 amount of RPP produced throughout the photoperiod did not differ.
321

322 The amount of DNP was generally much greater than that of RPP, especially during the
323 scotophase (Fig. 1a). It also showed much greater change over time (both with
324 photoperiod and age), varying from a mean of 9.6±1.9 to 105.2±25.0 ng/female. This
325 difference was most noticeable between titers in the photophase and (especially middle of
326 the) scotophase, in accord with previous studies on native pheromone titer in *H. virescens*
327 and many other species of moths (e.g., Foster, 2005b; Groot, 2014; Heath et al., 1991;
328 McNeil, 1991). ANCOVA, with amount of DNP as the dependent variable, revealed
329 highly significant effects for both time of photoperiod ($F_{5,65} = 5.96$, $p < 0.001$) and age
330 ($F_{1,65} = 27.4$, $p < 0.001$). There was a strong correlation ($F_{1,70} = 40.2$, $P<0.001$; $R^2 = 0.36$)
331 between RPP and logDNP (Fig. 1b).
332
333 ANCOVA with precursor enrichment (Fig. 1c) as the dependent variable showed no
334 effect of photoperiod ($F_{5,65} = 1.89$, $p = 0.11$), but an effect of age ($F_{1,65} = 10.2$, $p = 0.002$),
335 consistent with decreasing levels of native hemolymph trehalose in older females (Foster
336 et al., 2014).
337
338
339 *3.3. Effect of decapitation*
340 In the first 6 h after decapitation, DNP and RPP exhibited different patterns (Fig. 2a).
341 DNP showed a rapid and significant decrease (ANOVA, $F_{7,31} = 4.87$, $p<0.001$) from ca.
342 20 to 1.5 ng/female, consistent with the known effect of decapitation on total pheromone
343 titer in decapitated females (Eltahlawy et al., 2007). The mean amounts of DNP 4 and 6 h
344 after decapitation were lower (Tukey-Kramer HSD test) than the amounts prior to, or

345 0.25 h after, decapitation. By contrast, the mean amount of RPP did not change over the
346 first 6 h of decapitation (ANOVA, $F_{7,31} = 0.73$, $p = 0.65$), ranging from 5.3–8.8
347 ng/female. Twenty four hours after decapitation, both DNP and RPP titers had declined
348 to very low levels, both lower (ANOVA, $F_{1,11} = 11.4$, $P = 0.006$ and $F_{1,11}=12.3$, $P =$
349 0.005, respectively) than their respective values before decapitation.
350
351 Precursor enrichment did not change over the first 6 h following decapitation (ANOVA,
352 $F_{7,31} = 0.75$, $P = 0.63$; Fig. 2b). However, after 24 h of decapitation, precursor enrichment
353 was slightly greater ($F_{1,11}=10.6$, $P = 0.008$) than that prior to decapitation (Fig. 2b).
354
355 With regard to fatty acyl stores, females decapitated for 6 h had a lower titer (ANOVA,
356 $F_{2,19} = 7.32$, $P = 0.004$; Tukey-Kramer HSD test) of labeled Z11-16:Acyl than did intact
357 females at the start of the scotophase or intact females 6 h into the scotophase (Fig. 2c).
358 Titers of unlabeled Z11-16:Acyl in females decapitated 6 h were similar to those in intact
359 females 6 h into the scotophase, but less than those in females at the start of the
360 scotophase (ANOVA $F_{2,19} = 6.15$, $P = 0.004$; Tukey-Kramer HSD test; Fig. 2c). Of note
361 is that 6 h of decapitation over this period yielded similar ratios of labeled to unlabeled
362 Z11-16:Acyl as at the start of the scotophase (in intact females), whereas leaving females
363 intact over this period (i.e., through the scotophase) resulted in a relative decline in the
364 amount of unlabeled Z11-16:Acyl (compared to labeled Z11-16:Acyl) over the 6 h of the
365 scotophase.
366

For both labeled (ANOVA, $F_{2,19} = 0.56$, $P = 0.58$) and unlabeled 16:Acyl (ANOVA, $F_{2,19} = 0.56$, $P = 0.58$), there were no differences in titer among any of the treatments (Fig. 2d). In contrast to the similar amounts of unlabeled and labeled Z11-16:Acyl, the amount of unlabeled 16:Acyl was much greater than that of labeled 16:Acyl, indicating a relatively slow turnover of this very large pool.

*3.4. Effect of PBAN*

Injection of PBAN into females decapitated 16 h earlier led to a rapid increase (ANOVA, $F_{5,42} = 8.38$, $P<0.001$) in DNP (Fig. 3a), such that 1 h after injection the amount of DNP was greater (Tukey-Kramer HSD test) than that prior to injection (i.e., at t = 0). DNP increased throughout the 4 h of the experiment, although the amount 4.0 h after PBAN injection was not different to that 1.5 h after injection (Tukey-Kramer HSD test). Injection of PBAN also resulted in an initial small increase (ANOVA, $F_{5,42} = 3.36$, $P = 0.012$) in RPP (Fig. 3a), with the amount 1 h after injection being greater (Tukey-Kramer HSD test) than that prior to injection. After that, the level of RPP plateaued. The amount of RPP was always much less than that of DNP in females injected with PBAN. Precursor enrichment (Fig. 3b) showed a small change over the experiment (ANOVA, $F_{5,42} = 2.45$, $P = 0.049$), with enrichment 4 h after injection of PBAN being greater than that 0.25 h after injection (Tukey-Kramer HSD test).

Injection of PBAN stimulated a large increase (ANOVA, $F_{4,39} = 337.7$, $P<0.001$) in labeled Z11-16:Acyl (Fig. 3c); 4 h after injection, females had more (Tukey-Kramer HSD test) labeled Z11-16:Acyl than did females of all other treatments (which were similar).

The amount of unlabeled Z11-16:Acyl increased slightly with PBAN injection (ANOVA, $F_{4,39} = 3.41$, $P = 0.018$), with the amount 4 h after PBAN injection being greater (Tukey-Kramer HSD test) than that prior to injection (i.e., at t = 0). Neither labeled ($F_{4,39} = 2.24$, $P = 0.083$) nor unlabeled ($F_{4,39} = 1.77$, $P = 0.15$) 16:Acyl titers changed with PBAN injection (Fig. 3d).

## 4. Discussion

### *4.1. Identification of two pathways*

Through feeding $^{13}$C-labeled glucose to female *H. virescens,* we demonstrated that females produce two pools of pheromone: DNP, which incorporates $^{13}$C-tracer, and RPP, which does not. At most times, especially during the scotophase, the titer of DNP was much larger than that of RPP and, importantly, their respective titer profiles differed with regard to photoperiod and presence/absence of PBAN. The photoperiodic pattern of DNP titer closely resembled that of native titer in *H. virescens* (Foster, 2005b; Heath et al., 1991) and other moths (Groot, 2014; McNeil, 1991), with a substantial difference between the sexually inactive (photophase, titer low) and active (scotophase, titer high) periods. By contrast, RPP titer was constant throughout the photoperiod. For DNP (and native pheromone) this photoperiodic variation is explained by the presence/absence of PBAN acting on the gland (Eltahlawy et al., 2007; Groot et al., 2005; Rafaeli and Jurenka, 2003). RPP titer was largely independent of the presence/absence of PBAN, although females decapitated for ca. 16–24 h showed a small decline in RPP, which could be rectified by injection of PBAN. This, together with the concomitant changes in

413 precursor enrichment, showing a small decline in fat usage for DNP, suggest that
414 extended absence of PBAN, or perhaps another effect of decapitation, may result in other
415 (than fat and pheromone synthesis) minor effects on fat metabolism in the gland. The
416 small effect of age on both DNP and RPP is consistent with a senescent decline in
417 biosynthetic capability in the gland (Foster, 2005b; Raina et al., 1986)
418
419 The incorporation of $^{13}$C-label into DNP and its lack of incorporation into RPP, show the
420 two pools of pheromone must be biosynthesized by distinct, but related, routes (Fig. 4).
421 In our experiments, Z11-16:Ald DNP was biosynthesized de novo, after females fed on
422 labeled glucose. This route involves a cytosolic pool of labeled/unlabeled acetyl CoA,
423 formed from glycolysis/pyruvate oxidation and β-oxidation of stored fatty acids (Foster
424 and Anderson, 2015), and synthesis of transient 16:Acyl and Z11-16:Acyl precursors
425 (Fig. 4) (Choi et al., 2005). Since label from glucose is incorporated into pheromone very
426 rapidly after feeding (Foster and Anderson, 2011), the lack of label in RPP, at least 16 h
427 after feeding, shows that it cannot be produced from the same cytosolic acetyl CoA pool.
428 Instead, it must be derived largely from precursors in the female before adult feeding
429 (i.e., from nutrients acquired during larval feeding).
430
431 As suggested previously (Foster and Anderson, 2015), the most likely candidates for a
432 precursor of RPP are glandular glycerolipid stores of the pheromone precursor(s), Z11-
433 16:Acyl, 16:Acyl, and perhaps 18:Acyl. These acids are stored predominantly in
434 triacylglycerols in the gland, mostly on *sn*-1 and *sn*-3 positions of the glycerol backbone
435 (Foster, 2005b). Following hydrolysis by glandular lipases, these precursor acids can be

converted directly to pheromone (Choi et al., 2005; see also Fig. 4). Therefore, assuming pheromone gland lipases (Du et al., 2012) are typical triacylglycerol lipases, with little selectivity toward acyl groups of similar chain length (Watt and Steinberg, 2008), then the most probable precursor for production of RPP in our experiments, by virtue of its much greater abundance (Foster, 2005b; see also, Figs. 2b, 3b), is unlabeled 16:Acyl, although unlabeled 18:Acyl may also contribute. Stored Z11-16:Acyl probably contributes little to RPP measured in our experiments, since its isotopic enrichment was similar to that of pheromone (see also Foster et al., 2014). Hence, hydrolysis of stores of this moiety and conversion to pheromone, while strictly speaking also forming "recycled precursor fat" pheromone, will yield apparent increases in DNP from the isotopomer patterns. The much larger amount of stored 16:Acyl relative to Z11-16:Acyl, combined with the small production of RPP from 16:Acyl, suggests that only a small amount of DNP measured in our experiments was produced from stored Z11-16:Acyl. This may account for the small amount of "apparent" DNP observed throughout the photophase in our experiments, although it is possible that this is produced by a low level of de novo production in the absence of PBAN.

*4.2. PBAN control*

The small amount of RPP compared to the large amount of 16:Acyl (and to a lesser extent, Z11-16:Acyl) available in the gland of female *H. virescens* suggests limited but constant lipolysis that is largely independent of PBAN, in contrast to the situation in *B. mori* (Du et al., 2012; Matsumoto, 2010). However, during PBAN stimulation in *H. virescens*, acyl CoAs are also used for β-oxidation, producing acetyl CoA precursor for

459 DNP (Foster and Anderson, 2015), and perhaps for energy for cell function. Since fats
460 are used to produce up to one third of precursor for DNP (Foster and Anderson, 2015), it
461 is likely that there is considerably more lipolysis than indicated by RPP production alone.
462 When PBAN is absent, the likely fate of most acyl CoAs is re-esterification but when
463 present, most or a significant portion of liberated acyl CoAs is β-oxidized. During PBAN
464 stimulation, acyl CoAs may be compartmentalized, with de novo-synthesized acyl CoAs
465 (16:Acyl) being primarily converted directly to pheromone, while hydrolyzed, stored acyl
466 CoAs are β-oxidized, producing precursor for de novo synthesis. We do not suggest that
467 PBAN directly controls the flux of fatty acids into the mitochondria. Rather, it likely
468 controls this flux indirectly, as well as glycolytic flux, by controlling a downstream
469 process, such as conversion of acetyl CoA to malonyl CoA by acetyl CoA carboxylase
470 (Eltahlawy et al., 2007; Rafaeli and Jurenka, 2003)
471
472 Compartmentalization of different sources of acyl CoAs with different metabolic fates is
473 well established. In mice, the enzymes glycerol-3-phosphate acyltransferase (GPAT) and
474 carnitine palmitoyl transferase (CPT) compete for acyl CoAs at the outer mitochondrial
475 membrane, with GPAT preferentially loading de novo-synthesized acyl CoAs for
476 incorporation into glycerolipids, while CPT preferentially loads acyl CoAs from
477 glycerolipids for carnitine esterification and transport across the mitochondrial membrane
478 for β-oxidation (Cooper et al., 2015). This compartmentalization of newly synthesized
479 and stored fats is supported by our FAME experiments. Six hours after decapitation, both
480 labeled and unlabeled Z11-16:Acyl stores had declined by similar amounts; females
481 continue to use stores but cannot replenish them since they are not synthesizing new fatty

482 acids. By contrast, only unlabeled Z11-16:Acyl stores declined in intact females over the
483 same period; both labeled and unlabeled stores were utilized as in decapitated females,
484 but labeled stores were replenished via the tracer/tracee pool. In females injected with
485 PBAN, there was an expected increase in labeled Z11-16:Acyl stores, but also a small
486 increase in unlabeled stores, but only to levels similar to those prior to decapitation.
487
488 These trends were not apparent in 16:Acyl stores, perhaps because the amounts are much
489 greater and less subject to apparent change, and also because our dissections of glands
490 almost certainly contained other tissue in which 16:Acyl was abundant, masking any
491 effects peculiar to the gland.
492
493 *4.3. Contribution of stored fat to pheromonal communication*
494 The fact that a small amount of RPP is constantly produced throughout the entire
495 photoperiod, regardless of whether DNP is being synthesized or not, suggests that its
496 production is largely a consequence of constant hydrolysis of fats from glycerolipids, for
497 either β-oxidation or re-esterification, with only a small portion of free precursor acyl
498 CoAs (predominantly 16:Acyl) reaching the endoplasmic reticulum for conversion to
499 pheromone (Hagström et al., 2013). Furthermore, the amount of pheromone produced
500 directly (RPP route) by female *H. virescens* from stored precursor fats is relatively small,
501 especially in comparison to the amount of DNP produced during the sexually active
502 period. Therefore, RPP is likely, at best, to make a small contribution to the pheromone
503 released, especially for younger females attracting males for their first mating.
504

505 This dual pathway of pheromone production has been established, so far, only for *H*.
506 *virescens*. Hence, we do not know whether or not RPP contributes more or less to
507 pheromone production and release in other species of moths. Its contribution likely
508 depends on the amounts of pheromone precursor acids stored, as well as glandular
509 lipolytic activity. In the case of *B*. *mori*, females appear to produce all their pheromone
510 from precursor acyl CoAs hydrolyzed from triacylglycerols. However, photoperiodic
511 control of pheromone biosynthesis is somewhat unusual in this species, in that release of
512 PBAN appears to control fatty acid reduction (Matsumoto, 2010), rather than fatty acid
513 synthesis, as found for *H*. *virescens* (Eltahlawy et al., 2007) and other moths studied
514 (Rafaeli and Jurenka, 2003). Thus, fats are synthesized and stored in the absence of
515 PBAN, but not mobilized and reduced to pheromone until PBAN is released (Matsumoto,
516 2010). By contrast, in *H*. *virescens*, new precursor acyl CoAs are synthesized only when
517 DNP is also being produced, with only a small portion being stored in triacylglycerols;
518 their primary fate being pheromone (Foster and Anderson, 2012). It is also worth noting
519 that *H*. *virescens* adults feed (on nectar) and hence can replenish carbohydrate used
520 throughout the adult life; more than two thirds of acetyl CoA precursor for DNP
521 production in *H*. *virescens* is derived from hemolymph carbohydrate (trehalose) (Foster
522 and Anderson, 2015). Many species of moths, including *B*. *mori*, do not feed as adults
523 and hence may be more dependent upon stored fats for pheromone production, as both
524 DNP and RPP. Studying nutrient use for pheromone production across a range of species,
525 with different life history traits, is needed to determine whether recycling of stored
526 precursor fats is more than a minor route for contributing to pheromone production in
527 moths.

**Acknowledgments**

This work was funded in part by USDA Hatch Project ND02388. The purchase of the GC/MS system was funded in part by a USDA-NIFA Instrument Grant (2015-07238).

533
534 REFERENCES CITED


535 Allison, J.D., Cardé, R.T., 2016. Pheromone communication in moths: evolution,
536 behavior and application. University of California Press, Oakland, California, p. 401.
537
538 Ando, T., Inomata, S., Yamamoto, M., 2004. Lepidopteran sex pheromones., in: Schulz,
539 S. (Ed.), The Chemistry of Pheromones and Other Semiochemicals I. Springer Berlin /
540 Heidelberg, pp. 51-96.
541
542 Bjostad, L.B., Wolf, W.A., Roelofs, W.L., 1981. Total lipid analysis of the sex
543 pheromone gland of the redbanded leafroller moth, *Argyrotaenia velutinana*, with
544 reference to pheromone biosynthesis. Insect Biochem. 11, 73-79.
545
546 Bjostad, L.B., Wolf, W.A., Roelofs, W.L., 1987. Pheromone biosynthesis in
547 lepidopterans: desaturation and chain shortening., in: Prestwich, G.D., Blomquist, G.J.
548 (Eds.), Pheromone Biochemistry. Academic Press, New York, pp. 77-120.
549
550 Blomquist, G.J., Jurenka, R., Schal, C., Tittiger, C., 2011. Pheromone production:
551 biochemistry and molecular biology, in: Gilbert, L.I. (Ed.), Insect Endocrinology.
552 Academic Press, San Diego, CA, pp. 523-567.
553
554 Choi, M.Y., Groot, A., Jurenka, R.A., 2005. Pheromone biosynthetic pathways in the
555 moths *Heliothis subflexa* and *Heliothis virescens*. Arch Insect Biochem Physiol 59, 53-
556 58.
557
558 Du, M., Yin, X., Zhang, S., Zhu, B., Song, Q., An, S., 2012. Identification of Lipases
559 Involved in PBAN Stimulated Pheromone Production in *Bombyx mori* Using the DGE
560 and RNAi Approaches. PLoS ONE 7, e31045.
561
562 Eltahlawy, H., Buckner, J.S., Foster, S.P., 2007. Evidence for two-step regulation of
563 pheromone biosynthesis by the pheromone biosynthesis-activating neuropeptide in the
564 moth *Heliothis virescens*. Arch Insect Biochem Physiol 64, 120-130.
565
566 Fang, N., Teal, P.E.A., Tumlinson, J.H., 1995. PBAN regulation of pheromone
567 biosynthesis in female tobacco hornworm moths, *Manduca sexta* (L.). Arch Insect
568 Biochem Physiol 29, 35-44.
569
570 Foster, S., Anderson, K., 2011. The use of mass isotopomer distribution analysis to
571 quantify synthetic rates of sex pheromone in the moth *Heliothis virescens*. J Chem Ecol
572 37, 1208-1210.
573
574 Foster, S.P., 2004. Fatty acid and sex pheromone changes and the role of glandular lipids
575 in the Z-Strain of the European corn borer, *Ostrinia nubilalis* (Hübner). Arch Insect
576 Biochem Physiol 56, 73-83.

Foster, S.P., 2005a. The fate of topically applied fatty acids in the sex pheromone gland of the moth *Heliothis virescens*. Insect Biochemistry and Molecular Biology 35, 1021-1031.

Foster, S.P., 2005b. Lipid analysis of the sex pheromone gland of the moth *Heliothis virescens*. Arch Insect Biochem Physiol 59, 80-90.

Foster, S.P., 2016. Toward a quantitative paradigm for sex pheromone production in moths., in: Allison, J.D., Cardé, R.T. (Eds.), Pheromone communication in moths: evolution, behavior and application. University of California Press, Oakland,, CA, pp. 113-126.

Foster, S.P., Anderson, K.G., 2012. Synthetic rates of key stored fatty acids in the biosynthesis of sex pheromone in the moth *Heliothis virescens*. Insect Biochemistry and Molecular Biology 42, 865-872.

Foster, S.P., Anderson, K.G., 2015. Sex pheromones in mate assessment: analysis of nutrient cost of sex pheromone production by females of the moth *Heliothis virescens*. The Journal of Experimental Biology 218, 1252-1258.

Foster, S.P., Anderson, K.G., Harmon, J.P., 2014. Increased allocation of adult-acquired carbohydrate to egg production results in its decreased allocation to sex pheromone production in mated females of the moth *Heliothis virescens*. The Journal of Experimental Biology 217, 499-506.

Groot, A.T., 2014. Circadian rhythms of sexual activities in moths: a review. Frontiers in Ecology and Evolution 2.

Groot, A.T., Dekker, T., Heckel, D.G., 2016. The Genetic Basis of Pheromone Evolution in Moths. Ann Rev Entomol 61, 99-117.

Groot, A.T., Fan, Y., Brownie, C., Jurenka, R.A., Gould, F., Schal, C., 2005. Effect of PBAN on pheromone production by mated *Heliothis virescens* and *Heliothis subflexa* females. J Chem Ecol 31, 15-28.

Hagström, Å.K., Walther, A., Wendland, J., Löfstedt, C., 2013. Subcellular localization of the fatty acyl reductase involved in pheromone biosynthesis in the tobacco budworm, Heliothis virescens (Noctuidae: Lepidoptera). Insect Biochemistry and Molecular Biology 43, 510-521.

Heath, R.R., McLaughlin, J.R., Proshold, F., Teal, P.E.A., 1991. Periodicity of female sex pheromone titer and release in *Heliothis subflexa* and *H. virescens* (Lepidoptera: Noctuidae). Ann. Entomol. Soc. Am. 84, 182-189.

621 Hellerstein, M.K., Neese, R.A., 1992. Mass isotopomer distribution analysis: a technique
622 for measuring biosynthesis and turnover of polymers. American Journal of Physiology -
623 Endocrinology And Metabolism 263, E988-1001.
624
625 Hellerstein, M.K., Neese, R.A., 1999. Mass isotopomer distribution analysis at eight
626 years: theoretical, analytic, and experimental considerations. American Journal of
627 Physiology - Endocrinology And Metabolism 276, E1146-1170.
628
629 Ma, P.W.K., Ramaswamy, S.B., 2003. Biology and ultrastructure of sex pheromone-
630 producing tissue., in: Blomquist, G.J., Vogt, R.C. (Eds.), Insect pheromone biochemsitry
631 and molecular biology. Elsevier Academic Press., London, pp. 19-51.
632
633 Matsumoto, S., 2010. Molecular mechanisms underlying sex pheromone production in
634 moths. Bioscience, Biotechnology, and Biochemistry 74, 223-231.
635
636 McNeil, J.N., 1991. Behavioral ecology of pheromone-mediated communication in moths
637 and its importance in the use of pheromone traps. Ann Rev Entomol 36, 407-430.
638
639 Rafaeli, A., Jurenka, R., 2003. PBAN regulation of pheromone biosynthesis in female
640 moths, in: Blomquist, G.J., Vogt, R.C. (Eds.), Insect Pheromone Biochemistry and
641 Molecular Biology. Elsevier, Amsterdam, pp. 107-136.
642
643 Raina, A.K., Klun, J.A., Stadelbacher, E.A., 1986. Diel periodicity and effect of age and
644 mating on female sex pheromone titer in *Heliothis zea* (Lepidoptera: Noctuidae). Ann.
645 Entomol. Soc. Am. 79, 128-131.
646
647 Roelofs, W.L., Hill, A.S., Cardé, R.T., Baker, T.C., 1974. Two sex pheromone
648 components of the tobacco budworm moth, *Heliothis virescens*. Life Sci 14, 1555-1562.
649
650 Teal, P.E.A., Tumlinson, J.H., Heath, R.R., 1986. Chemical and behavioral analyses of
651 volatile sex pheromone components released by calling *Heliothis virescens* (F.) females
652 (Lepidoptera: Noctuidae). J Chem Ecol 12, 107-126.
653
654 Watt, Matthew J., Steinberg, Gregory R., 2008. Regulation and function of
655 triacylglycerol lipases in cellular metabolism. Biochemical Journal 414, 313-325.
656
657 Wolfe, R.R., Chinkes, D.L., 2005. Isotope Tracers in Metabolic Research, Second
658 Edition. John Wiley & Sons, Inc.
659

660
661 **Captions**

662 **Figure 1. Mean titers (±SEM) of de novo-produced pheromone (DNP) and recycled**
663 **precursor fat pheromone (RPP) in female *Heliothis virescens* of different age and**
664 **times of the photoperiod.** a) DNP and RPP. (b) Relation between DNP (log scale) and
665 RPP titers. (c) Pheromone precursor enrichment (in molar percent excess; MPE) of DNP.
666 Age of female (in days) given below figures. Numbers above bars are numbers of
667 replicates.

668

669 **Figure 2. Mean titers (±SEM) of various pheromone-related moieties in female**
670 ***Heliothis virescens* fed U-$^{13}$C-glucose the previous day and decapitated at the start of**
671 **the subsequent scotophase.** A) De novo-produced pheromone (DNP) and recycled
672 precursor fat pheromone (RPP). (b) Pheromone precursor enrichment (in molar percent
673 excess; MPE) of DNP. Labeled and unlabeled (c) (*Z*)-11-hexadecenoate (Z11-16:Acyl)
674 and (d) hexadecanoate (16:Acyl). Decap6 = decapitated (at S0) for 6 h. Different letters
675 (of the same case) above bars indicate means that are different ($P<0.05$, Tukey-Kramer
676 test), while numbers in parentheses are the numbers of replicates.

677

678 **Figure 3. a) Mean titers (±SEM) of various pheromone-related moieties in**
679 **decapitated female *Heliothis virescens* fed U-$^{13}$C-glucose and analyzed following**
680 **injection with pheromone biosynthesis-activating neuropeptide (PBAN).** a) De novo-
681 produced pheromone (DNP) and recycled precursor fat pheromone (RPP). (b) Pheromone
682 precursor enrichment (in molar percent excess; mpe) for DNP. Labeled and unlabeled (c)
683 (*Z*)-11-hexadecenaoate (Z11-16:Acyl) and (d) hexadecanoate (16:Acyl). Letters above

bars indicate means that are different ($P<0.05$, Tukey-Kramer test), while numbers in parentheses are numbers of replicates.

**Figure 4. Biosynthesis of pheromone [(*Z*)-11-hexadecenal] in the gland of *Heliothis virescens* females by two distinct routes: de novo-produced pheromone (DNP) and recycled precursor fat pheromone (RPP).** Processes that occur throughout the day have grey arrows, while processes that occur primarily during the sexually active period (scotophase) have black arrows. Features are: (1) stored acyl CoAs are continuously hydrolyzed and re-esterified to glycerolipids, (2) DNP production is controlled by release of pheromone biosynthesis activating neuropeptide (PBAN) from the corpora cardiaca, which acts on a step in de novo synthesis of hexadecanoate (16:Acyl), and (3) this indirectly controls fluxes of β-oxidation of glandular fats and glycolysis/pyruvate oxidation of glucose (from hemolymph trehalose) to produce acetyl CoA precursor. Z11-16:Acyl is the pheromone precursor acid (*Z*)-11-hexadecenoate.

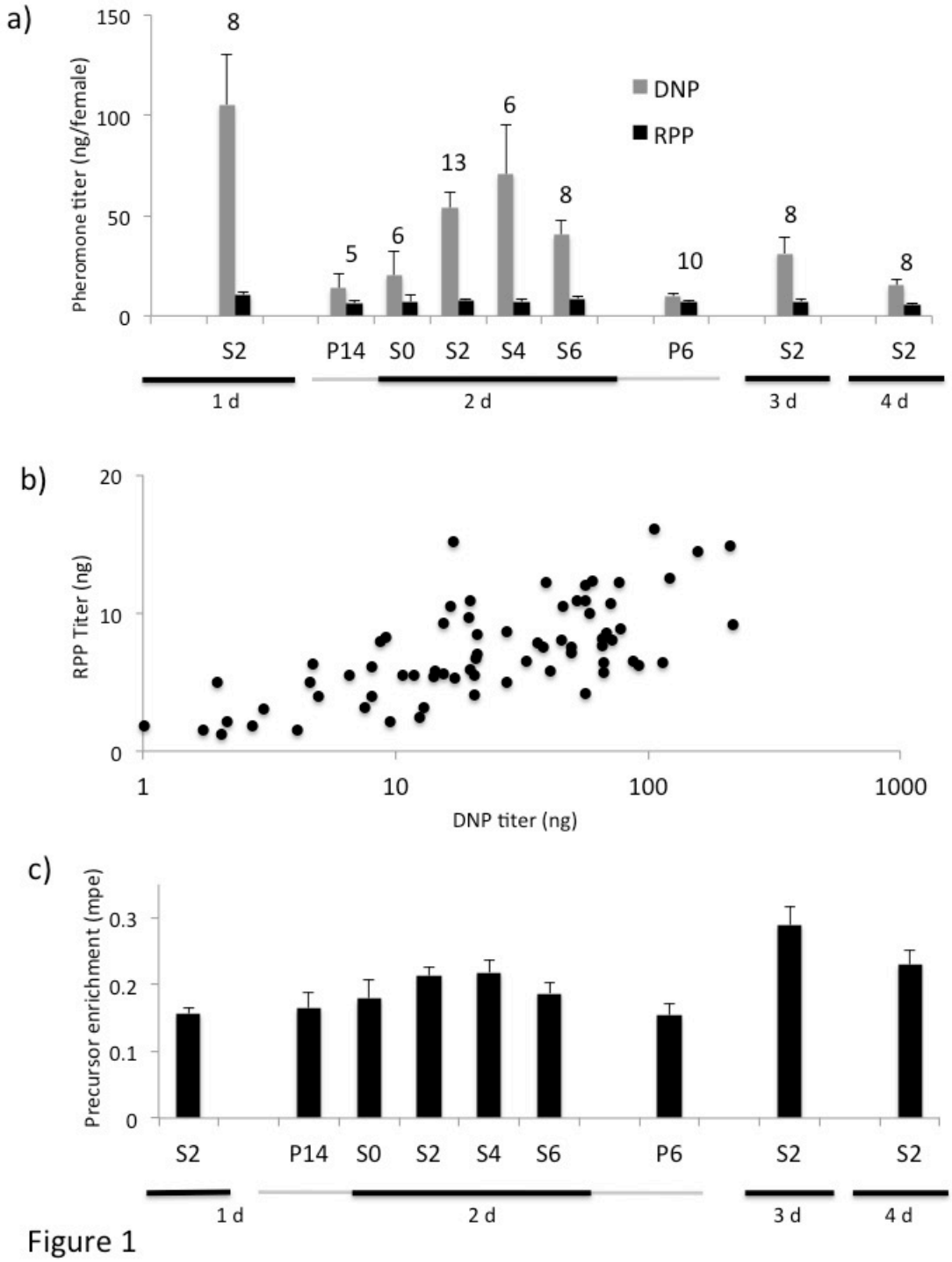
a)
Pheromone titer (ng/female)
150
100
50
0
DNP
RPP
8
5
6
13
6
8
10
8
8
S2
P14
S0
S2
S4
S6
P6
S2
S2
1 d
2 d
3 d
4 d
b)
RPP Titer (ng)
20
10
0
1
10
100
1000
DNP titer (ng)
c)
Precursor enrichment (mpe)
0.3
0.2
0.1
0
S2
P14
S0
S2
S4
S6
P6
S2
S2
1 d
2 d
3 d
4 d

Figure 1

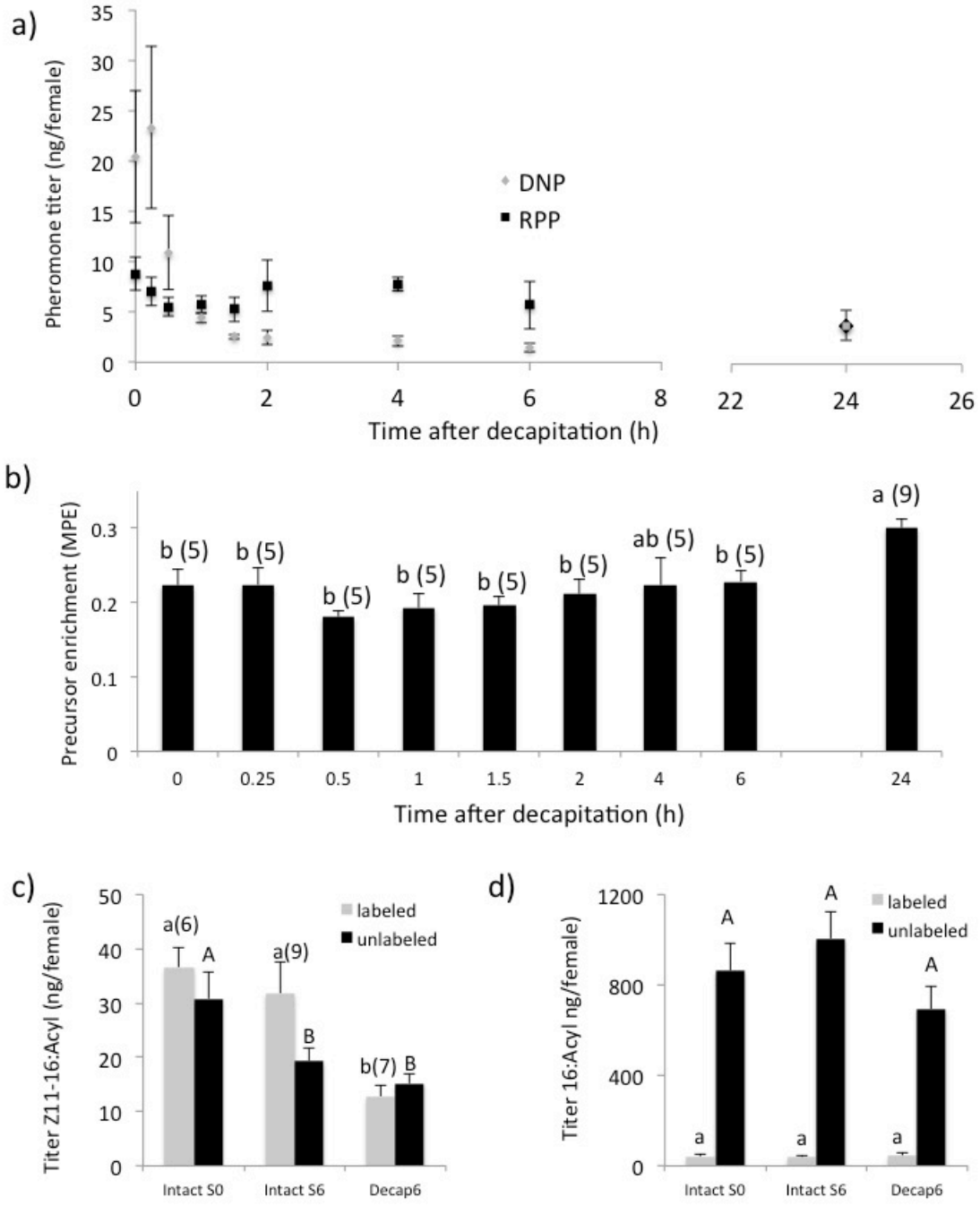
a)
Pheromone titer (ng/female)
DNP
RPP
Time after decapitation (h)
b)
Precursor enrichment (MPE)
b (5)
b (5)
b (5)
b (5)
b (5)
b (5)
ab (5)
b (5)
a (9)
Time after decapitation (h)
c)
Titer Z11-16:Acyl (ng/female)
labeled
unlabeled
a(6)
A
a(9)
B
b(7) B
Intact S0
Intact S6
Decap6
d)
Titer 16:Acyl ng/female)
labeled
unlabeled
A
A
A
a
a
a
Intact S0
Intact S6
Decap6

Figure 2

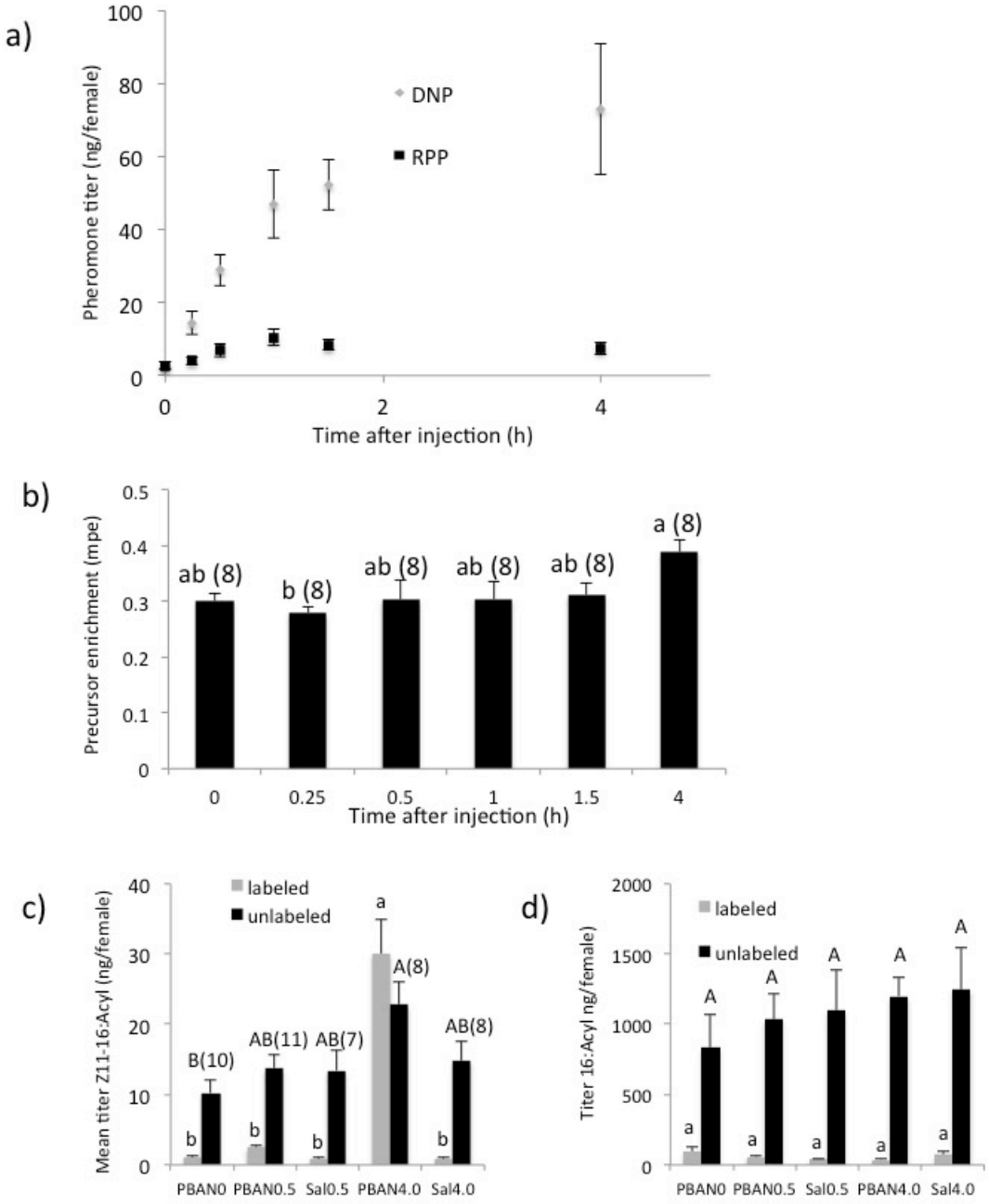


Figure 3

709
710

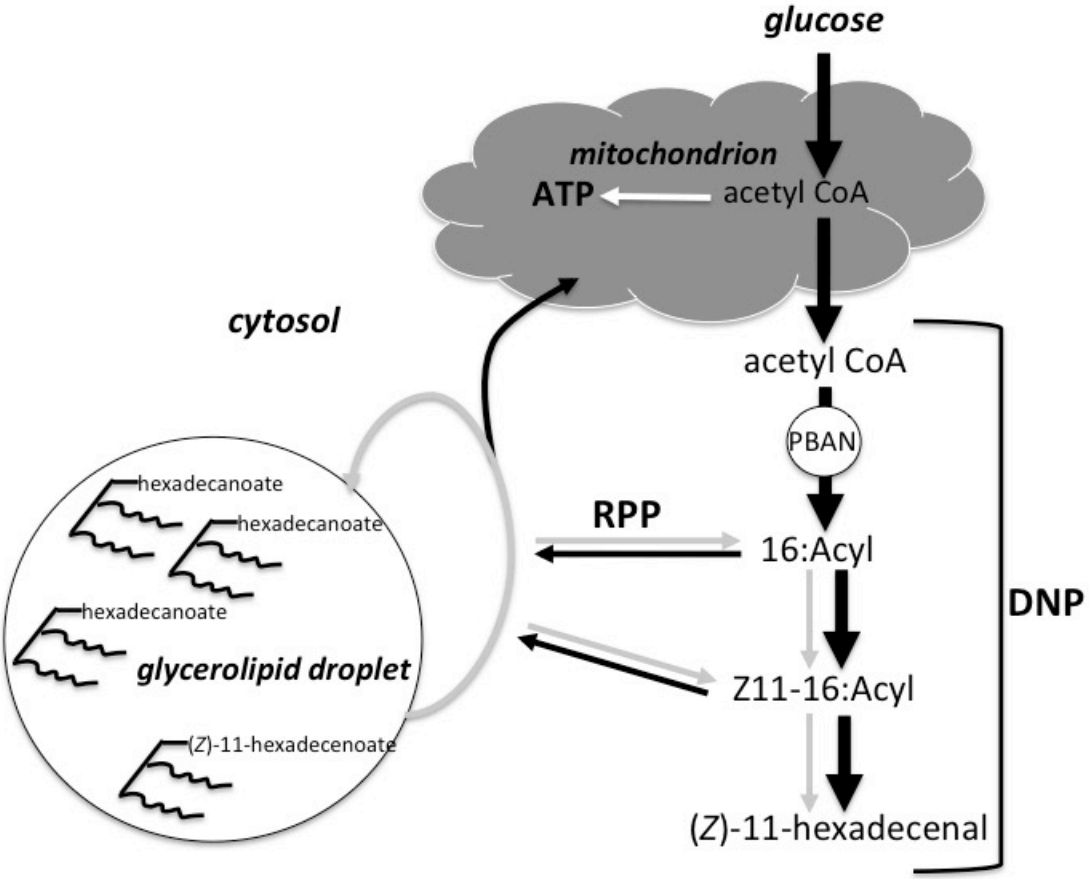
glucose
mitochondrion
ATP
acetyl CoA
cytosol
acetyl CoA
PBAN
RPP
16:Acyl
DNP
hexadecanoate
hexadecanoate
hexadecanoate
glycerolipid droplet
(Z)-11-hexadecenoate
Z11-16:Acyl
(Z)-11-hexadecenal

Figure 4

711